Research Square

Preprints are preliminary reports that have not undergone peer review.
They should not be considered conclusive, used to inform clinical practice,
or referenced by the media as validated information.

Induction of a Regenerative State in Hair Follicle Stem Cells by Helium Plasma-Activated Medium Through Coordinated Regulation of Regenerative Programs

Kamal Hajisharifi
hajisharifi@khu.ac.ir

Kharazmi University

Sara Emadi
Kharazmi University

Elaheh Amini
Kharazmi University

Hassan Mehdian
Kharazmi University

Sareh Pandamooz
Shiraz University

Erfan Tamandeh
Kharazmi University

Eric Robert
UMR 7344 GREMI, CNRS/Université d'Orléans

Research Article

Keywords: cold atmospheric plasma, plasma-activated medium, hair follicle stem cells, gene expression, regeneration, wound healing

Posted Date: September 18th, 2026

DOI: https://doi.org/10.21203/rs.3.rs-10437201/v1

License: This work is licensed under a Creative Commons Attribution 4.0 International License.
Read Full License

Additional Declarations: No competing interests reported.

Abstract

Hair follicle stem cells (HFSCs) are central regulators of hair follicle regeneration and tissue repair, requiring coordinated control of stem-cell activation, migratory responsiveness, and epithelial plasticity. Plasma-activated media have emerged as promising bioactive platforms for regenerative applications through the controlled delivery of reactive oxygen and nitrogen species. In this study, the biological effects of helium plasma-activated medium (He-PAM) on HFSCs were evaluated using functional and molecular analyses. Cell metabolic and migratory activity were assessed alongside the expression of genes associated with regenerative activation (RUNX1, LGR4, and CCND1), migratory competence (CXCR4), and epithelial plasticity (SNAI1 and OVOL2). The selected He-PAM significantly enhanced HFSCs metabolic activity and migration while inducing coordinated transcriptional changes across all three biological programs. Increased expression of RUNX1, LGR4, and CCND1 was associated with regenerative activation, CXCR4 upregulation supported enhanced migratory responsiveness, and the concurrent induction of SNAI1 and OVOL2 was consistent with a transcriptional pattern associated with epithelial plasticity. Collectively, these findings indicate that He-PAM promotes a regenerative-response profile in HFSCs characterized by coordinated regenerative activation, migratory competence, and epithelial plasticity, highlighting its potential as a plasma-based strategy for hair follicle regeneration and broader regenerative medicine application.

1. Introduction

Hair follicle stem cells (HFSCs), localized within the bulge region of the hair follicle, are responsible for follicular cycling, epidermal repair, and neuroectodermal regeneration [1, 2]. Owing to their self-renewal capacity and multipotency, HFSCs represent an attractive cellular source for regenerative medicine, especially for alopecia treatment and cutaneous wound repair [3, 4]. However, obtaining viable HFSCs in sufficient numbers remains technically challenging, as enzymatic dissociation methods can disrupt the follicular niche and compromise cell metabolic activity. Recent protocols employing microdissection and extracellular matrix coatings have improved isolation efficiency and stemness maintenance [5].

Recent advances in hair follicle biology have substantially expanded the understanding of the mechanisms governing the function of HFSCs during tissue homeostasis and regeneration. Emerging evidence indicates that effective follicular regeneration is not solely dependent on stem-cell proliferation, but rather requires the coordinated integration of multiple biological processes that collectively determine regenerative competence. Among these, activation of stem-cell regenerative programs is considered a prerequisite for hair-cycle re-entry and long-term follicular renewal, enabling HFSCs to transition from a quiescent state toward active participation in tissue regeneration [6, 7]. In parallel, the acquisition of migratory competence has emerged as a critical determinant of regenerative efficacy, as HFSCs must respond to environmental cues, relocate within damaged tissues, and contribute to wound repair and follicular reconstruction [8]. Furthermore, recent studies have highlighted epithelial plasticity as a fundamental feature of regenerative stem cells, allowing HFSCs to dynamically adapt their cellular state in response to niche-derived signals while preserving their regenerative identity. Controlled

transitions between epithelial and mesenchymal programs are now recognized as essential mechanisms underlying tissue remodeling, wound re-epithelialization, and successful follicular regeneration [9–11]. Collectively, these observations suggest that simultaneous evaluation of regenerative activation, migratory potential, and epithelial plasticity provides a biologically relevant framework for assessing the regenerative status of HFSCs and may offer valuable insight into the mechanisms through which emerging therapeutic interventions influence hair follicle regeneration.

Cold atmospheric plasma (CAP), a partially ionized gas near room temperature, generates a complex mixture of electrons, ions, UV photons, reactive oxygen and nitrogen species (RONS), and physical factors including transient electric fields, electromagnetic fields, charged species, and plasma-induced microcurrents, all of which contribute to biological responses without thermal injury [12–15]. Recent evidence indicates that CAP-induced biological responses arise from the interplay between RONS and these physical plasma components [14, 15]. When CAP interacts with liquids, it generates plasma-activated medium (PAM), containing bioactive species such as hydrogen peroxide, nitrites, and peroxynitrites that modulate cellular signaling pathways, including PI3K/AKT, MAPK, and Wnt/β-catenin, thereby acting as promising therapeutic platforms for tissue repair and regeneration [16–19]. Previous studies have demonstrated that direct CAP treatment or PAM exposure can enhance fibroblast proliferation, accelerate keratinocyte migration, and activate mesenchymal stem cell differentiation [20–22]. The dermal papilla cells are considered niche cells that regulate the behavior of hair follicle stem cells (HFSCs) residing in the bulge region. In this context, CAP stimulation has been shown to upregulate β-catenin and CCND1, key regulators of the hair growth cycle [23, 24]

Despite growing evidence supporting their regenerative potential in various cell types and tissues, the biological mechanisms through which plasma-derived reactive species influence the regenerative behavior of hair follicle stem cells (HFSCs) remain insufficiently understood. Considering the pivotal roles of regenerative activation, migratory competence, and epithelial plasticity in determining HFSCs function during follicular renewal and tissue regeneration, we hypothesized that helium plasma-activated medium (He-PAM) may modulate these interconnected biological programs and thereby influence the regenerative state of HFSCs. To address this hypothesis, cellular metabolic and migratory activity were evaluated in parallel with the expression of genes associated with stem-cell recruitment and migratory responsiveness (CXCR4), epithelial plasticity and dynamic cell-state transitions (SNAI1 and OVOL2), and regenerative activation pathways implicated in stem-cell competence, follicular renewal, and hair-cycle regulation (RUNX1, LGR4, and CCND1). Through the integration of functional and molecular analyses, this study aimed to provide functional and transcriptional insight into the biological responses of HFSCs to He-PAM and to evaluate its potential as a novel regenerative strategy for modulating key processes governing hair follicle regeneration.

2. Materials and Methods

2.1. Plasma Jet Fabrication and PAM Preparation

A custom-designed helium CAP jet consisted of a stainless-steel pin electrode (0.3 mm diameter, 15 cm length) coaxially aligned inside a quartz tube (ID 3 mm, OD 5 mm) with a copper ring electrode (5 mm width) near the outlet (Fig. 1) was used in this work. A sinusoidal voltage signal (9–14 kV, 14 kHz) was applied across the electrodes while helium flow was set at 1 slm. The distance between the tube nozzle and the liquid surface was fixed at 15 mm. To prepare PAM, 600 µL of serum-free α-MEM was exposed to CAP for 30 or 60 s and used within 30 min. Treatment conditions are summarized in Table 1.

Table 1
Voltage and duration conditions used for PAM preparation.

Time (s)	Voltage (kV)	Group ID
0	0	Control
30	9	t1
60	9	t2
30	10	t3
60	10	t4
30	11	t5
60	11	t6
30	12	t7
60	12	t8
30	13	t9
60	13	t10
30	14	t11
60	14	t12

2.2. HFSC Isolation, Culture, and Study Design

Hair follicle stem cells (HFSCs) were isolated from the vibrissal bulge region of Sprague–Dawley rats (30–35 g) using a modified protocol based on the methods described by Pandamooz et al. [2013] and Mousavi et al. [2022] [25, 26]. Hair follicle stem cells were isolated from whisker-pad tissues collected post-mortem from 3-week-old rats that had been euthanized by carbon dioxide (CO_2) inhalation for purposes unrelated to the present study. No chemical anesthetic was administered prior to euthanasia. Briefly, whisker pads were excised under sterile conditions, disinfected with 70% ethanol, and subsequently immersed in povidone–iodine (Betadine) solution for 3–5 min. Individual vibrissal follicles were then carefully dissected under a stereomicroscope, and the bulge regions were isolated using fine microsurgical needles. The explanted bulges were cultured on collagen type I–coated dishes (1 mg/mL, Roche; #11179179001) in α-minimum essential medium (α-MEM) supplemented with 10% fetal bovine

serum (FBS) and 10% chick embryo extract (CEE) and 1% penicillin/streptomycin (P/S). Cultures were maintained at 37°C in a humidified cell culture incubator containing 5% CO_2. Migratory cells emerged from the explants within 3–4 days and were expanded to passage 4 prior to experimental use.

2.3. Immunofluorescence Staining

To characterize the morphology, cytoskeletal organization, and stem/progenitor phenotype of cultured hair follicle stem cells (HFSCs), immunofluorescence staining was performed. HFSCs were seeded onto four-chamber glass slides at a density of 7.5×10^4 cells per chamber and cultured overnight. Cells were fixed by adding 4% paraformaldehyde (PFA) for 10 min at room temperature. After fixation, cells were washed three times with PBS containing 0.1% Tween-20 (PBS-T). Next, cells were blocked with blocking solution containing 0.1% Triton X-100, 1% fetal bovine serum (FBS), and 10% normal goat serum in PBS for 30 min at room temperature. For F-actin staining, cells were incubated with Alexa Fluor™ 488-conjugated phalloidin (1:200; Cell Signaling Technology, #8878) diluted in blocking solution for 1 h. For nestin immunostaining, cells were then incubated overnight at 4°C with mouse anti-nestin monoclonal antibody (1:50; Abcam, #ab6142). Next day, after three washes with PBS-T, cells were incubated with goat anti-mouse IgG Alexa Fluor™ 488 (1:1000; Thermo Fisher Scientific, #A-11001) for 2 h at room temperature. Cell nuclei were counterstained using ProLong™ Glass Antifade Mountant with NucBlue™ Stain (Invitrogen, #P36985), and coverslips were mounted prior to imaging. Fluorescence images were acquired using a Leica DM5000B epifluorescence microscope.

2.4. Cell Treatment and metabolic activity Assay

Approximately 1×10^4 cells per well were seeded into 96-well plates and incubated overnight to allow cell attachment. The culture medium was then replaced with 100 µL freshly prepared PAM at various parameters (voltage and frequency). Control wells received untreated α-MEM. Briefly, cells were incubated with MTT solution (5 mg/mL; Sigma Aldrich, USA; cat number: CT01/CT02) for 3 h at 37°C, after which the resulting formazan crystals were quantified by measuring the absorbance at 570 nm using a microplate reader (Bio-Rad, USA).

2.5. Scratch Migration Assay

HFSCs were cultured in 6-well plates until they reached approximately 85% confluence. The confluent monolayers were incubated with Mitomycin C (concentration of 5 µg/mL; Stemcell Technologies, Canada; cat number: 73274 100–1048) for 2 h at 37°C (Mouritzen and Jenssen 2018). After aspiration, the confluent monolayers were scratched with a sterile tip and rinsed with PBS. In order to assess migratory capacity, the cells were incubated with PAM prepared under six selected conditions (Table 2), chosen based on metabolic activity profiles (12–14 kV, 30–60 s). Wound-closure images were captured at 0 h and 48 h using an inverted microscope. The wound closure area was quantified using image J software, and the percentage of wound closure was calculated using the following formula:

Relative Wound Closure (%) = [(Initial width − Width at time X) / Initial width] × 100

Table 2
PAM treatment conditions selected for migration and gene-expression assays.

Time (s)	Voltage (kV)	Group ID
0	0	Control
30	12	t7
60	12	t8
30	13	t9
60	13	t10
30	14	t11

2.6. Quantitative Real-Time PCR (qRT-PCR)

Total RNA from treated and untreated HFSCs was extracted using a RNeasy Kits for RNA Purification kit (Qiagen; Cat. No.: 74104) according to the manufacturer's instructions. Complementary DNA (cDNA) was synthesized using the First Strand Reverse Transcription Kit (Qiagen, Cat. No.: 205311). Expression levels of *SNAI1*, *CXCR4*, *OVOL2*, *RUNX1*, *LGR4*, and *CCND1* were quantified by real time PCR. In this regard, 10 µL SYBR green mastermix,1 µL of forward primer, 1 µL of reverse primer, 1 µL cDNA, and 7 µL DEPC-treated water were mixed in 20 µL total volume and PCR reactions were performed in triplicate using a CFX-96 Real-Time PCR System (Bio-Rad, USA). GAPDH was used as internal reference gene (forward sequence: ATCACCATCTTCCAGGAGCGA; reverse sequence: AGCCTTCTCCATGGTGGTGGA). The primer sequences are listed in Table 3. The PCR cycling conditions were as follows: initial denaturation at 95^{o}C for 3 min, followed by 45 cycles at 95^{o}C for 10 seconds, annealing degree for 30 seconds and extension time for 20 seconds. The target gene expression level was calculated using the $2^{-\Delta\Delta CT}$ formula.

Table 3
List of primers used for assessment regenerative capacity of HFSCs.

Gene ID	Primer Seq (5'->3')	Tm	PCR Product (bp)
Snai1	AGTTGTCTACCGACCTTGCG	60.04	128
snail family transcriptional repressor 1	TGCAGCTCGCTATAGTTGGG	59.95	
Cxcr4	GGCGTTTGGTGCTCCGGTA	62.89	206
C-X-C motif chemokine receptor 4	TTGCCCACTATGCCAGTCAAG	60.61	
Ovol2	CGAGTAGCCGGGAGTGAAGG	62.01	192
ovo-like zinc finger 2	AGACTTTGGGCATGGTGGGA	61.43	
Runx1	CGGGACCGTTTGTAATAGCC	58.71	121
RUNX family transcription factor 1	GTTAGCAACTGGCCGCTTAG	59.27	
Lgr4x	ACCAGGGTGTTTGTGAGAACCC	62.67	93
leucine-rich repeat-containing G	AACCGCACGGCTCCTCAAG	62.88	
Ccnd1	CAAGTGTGACCCGGACTGC	60.96	209
cyclin D1	TACTTGGTGACTCCCGCCT	60.23	

Statistical analysis

All experiments were performed in triplicate, and the data are represented as mean ± standard deviation (SD). Data were analyzed using one-way ANOVA followed by Tukey's post hoc test. A p value of less than 0.05 was considered statistically significant.

3. Results

3.1. Morphological and Immunofluorescence Characterization of Hair Follicle Stem Cells

Hair follicle stem cells (HFSCs) were isolated from the bulge region of whisker hair follicles (Fig. 3A,B). Following culture, the cells exhibited a typical spindle-shaped, fibroblast-like morphology and formed a homogeneous adherent cell population (Fig. 3C). To further characterize the cultured cells, phalloidin staining revealed a well-organized filamentous actin (F-actin) cytoskeleton (Fig. 3D), while Hoechst staining demonstrated uniformly distributed nuclei (Fig. 3D'). The merged image confirmed the elongated morphology and intact cytoskeletal organization of the cultured cells (Fig. 3D''). Immunofluorescence analysis further demonstrated positive nestin expression in the cultured cells (Fig. 3E). Hoechst staining identified the cell nuclei (Fig. 3E'), and the merged image (Fig. 3E'') confirmed

nestin immunoreactivity in the majority of the cultured cells, supporting their stem/progenitor-like phenotype.

3.2. Cell metabolic activity

As shown in Fig. 4, most PAM-treated cells showed no significant cytotoxicity 24 h after treatment. Among the treatment groups, cells exposed to 11kV for 30s and 13 kV for 30s exhibited reduced HFSC metabolic activity (86.6%, 76.7%; *$p < 0.05$). Meanwhile, PAM treatments increased cell metabolic activity compared with the control group 48 h after treatment. Based on the MTT assay findings, the maximum HFSC metabolic activity was observed following exposure to 14 kV for 30s and 11 kV for 60s, reaching 151.3 and 151.9% of the control value, respectively (***$p < 0.001$). Statistical analysis confirmed meaningful differences among groups ($F = 4.70$, (***$p < 0.001$)). In contrast, HFSC metabolic activity decreased to 90.2% following exposure to 13 kV for 60s (48h post treatment).

3.3. Scratch assay

Representative scratch-assay images showed that He-PAM treatment promoted the migratory behavior of HFSCs. Microscopic images indicated that the degree of wound closure in t8 (12 kV, 60s) and t11 (14 kV, 30s) treatment groups after the scratch (0 hour) and 48 hours PAM exposure was higher than that observed in the t7, t9, t10 experimental groups (Fig. 5A). The image J analysis revealed that PAM (t8 and t11) significantly increased cell migration after 48h treatment. The relative wound closure was 59.8% in control, compared to 92.4% and 82.6% in HFSCs under exposure with PAM. These results demonstrate that both t8 (12 kV, 60 s) and t11 (14 kV, 30 s) significantly increased the migratory capacity of HFSCs compared with the control group **(**Fig. 5B**).**

3.4. Migratory and stemness gene-Expression analysis

As exhibited in Fig. 6, under exposure with Helium-PAM (t7, t8, t9, t10, t11) the expression of target genes changed compared with control. Among the investigated conditions, t11 (14 kV, 30 s) produced one of the most pronounced overall transcriptional responses, including the highest expression of CXCR4, SNAI1, OVOL2, LGR4, and CCND1. The highest level of gene expression was observed for *CXCR4* (5.86-fold change). Additionally, *OVOL2* and *LGR4* gene expression indicated 2.29-fold change, and 1.46-fold change, respectively 48h post treatment with t11, indicating enhanced regenerative and migratory potential under the t11 treatment condition. In this regard, the lowest degree of upregulation was observed for *LGR4* expression level under exposure with t11.

Table 4
Fold-change expression of target genes in HFSCs after PAM treatment.

Group	SNAI1 (Snail)	CXCR4	OVOL2	RUNX1	LGR4	CCND1
Control	1.000	1.000	1.000	1.000	1.000	1.000
t7	1.803	3.183	1.866	1.932	1.231	2.549
t8	2.071	3.249	2.219	1.803	1.320	3.605
t9	1.682	2.828	2.000	1.569	1.315	2.639
t10	1.366	2.219	1.366	1.066	1.072	2.07
t11	2.378	5.856	2.297	1.414	1.464	3.732

In addition, SNAI1 and CCND1 expression levels increased by 2.38-fold and 3.73-fold, respectively, following treatment with He-PAM at 14 kV for 30 s. These transcriptional changes indicate that the He-PAM response extends beyond genes associated with cell-cycle regulation and includes genes related to migratory responsiveness and epithelial plasticity. These transcriptional changes are consistent with modulation of genes associated with epithelial plasticity and Wnt-related regenerative regulation in HFSCs treated 14 kV, 30s Helium-PAM jet (Fig. 6). Fold changes are summarized in Table 4.

4. Discussion

This study provides evidence that He-PAM modulates HFSC metabolic activity, migration, and a regeneration-associated transcriptional profile. The biological responses of HFSCs to He-PAM were investigated with particular emphasis on genes associated with migration, epithelial–mesenchymal plasticity, and regenerative activation. In this regard, the aim of the present study was to investigate how PAM influences the transcriptional landscape of HFSCs, particularly regarding genes associated with migration, epithelial–mesenchymal plasticity (EMT/MET) and stem-cell renewal.

The present study demonstrates that He-PAM, generated by helium-based cold atmospheric plasma, exerts significant biological effects on hair follicle stem cells (HFSCs), as evidenced by enhanced cellular metabolic activity, increased migratory activity, and the induction of a regeneration-associated transcriptional profile. Among the investigated conditions, He-PAM generated at 14 kV for 30s showed one of the most consistent combined functional and transcriptional responses, suggesting that the regenerative effects of plasma-derived reactive species are highly dependent on treatment parameters. This observation is consistent with the growing concept of plasma-induced hormesis, whereby low and controlled levels of reactive oxygen and nitrogen species (RONS) function as signaling mediators that stimulate adaptive cellular responses, whereas excessive oxidative stimulation may compromise cellular function and survival. The variability observed among different He-PAM conditions, particularly the reduced metabolic activity observed under prolonged exposure parameters, further supports the importance of selecting plasma settings to achieve biologically beneficial outcomes. Based on established plasma–liquid chemistry, plasma-generated reactive species represent plausible mediators

of these responses; however, the composition of He-PAM was not directly characterized in the present study. In the context of HFSCs biology, successful regeneration requires not only maintenance of cell survival but also activation of molecular programs that enable stem cells to respond effectively to regenerative cues and participate in tissue renewal. Consistent with this concept, the increased metabolic activity observed following selected He-PAM treatment was accompanied by elevated expression of RUNX1, LGR4, and CCND1, genes that have been implicated in stem-cell competence, follicular regeneration, and hair-cycle re-entry [27–29]. Importantly, recent advances in HFSCs biology have increasingly emphasized that regenerative competence is governed by dynamic interactions between stem cells and their niche rather than by proliferative activity alone, highlighting the importance of stem-cell activation programs during tissue regeneration [6, 7]. Collectively, these findings suggest that selected He-PAM conditions may promote regenerative activation programs associated with enhanced stem-cell readiness and follicular renewal.

Beyond its effects on metabolic activity, the selected He-PAM significantly enhanced the migratory capacity of HFSCs, consistent with an enhanced regenerative-response profile and increased responsiveness to tissue-repair signals. This functional observation was accompanied by a pronounced upregulation of CXCR4, which represented the most strongly induced gene in the present study. CXCR4-mediated signaling plays a central role in stem-cell homing, chemotaxis, wound healing, and tissue regeneration through cellular responses to CXCL12 gradients [8, 30]. Therefore, the substantial increase in CXCR4 expression, together with the enhanced wound-closure rate observed in the scratch assay, suggests that He-PAM promotes biological programs associated with stem-cell recruitment, migratory responsiveness, and regenerative tissue remodeling. Previous studies have suggested that plasma-derived reactive species may influence redox-sensitive signaling networks, including PI3K/AKT, NF-κB, and TGF-β-associated pathways [13, 18]. Although these signaling cascades were not directly evaluated in the present study, the observed transcriptional and functional responses are consistent with the possibility that selected He-PAM modulates downstream pathways involved in cellular motility and regenerative responsiveness. Since effective tissue regeneration depends on the ability of stem cells to sense, migrate toward, and respond to regenerative microenvironments, the enhanced migratory competence observed following He-PAM exposure may represent an important component of its regenerative activity.

An additional and particularly noteworthy finding of this study was the simultaneous upregulation of SNAI1 and OVOL2. Traditionally, SNAI1 is recognized as a key regulator of epithelial-to-mesenchymal transition (EMT), promoting transient cellular motility and cytoskeletal remodeling required for tissue repair and re-epithelialization [31, 32]. In contrast, OVOL2 functions as an important regulator of mesenchymal-to-epithelial transition (MET) and contributes to the restoration of epithelial identity following regenerative remodeling [9, 33]. The concurrent induction of both factors does not support a simple interpretation of a unidirectional EMT response and is instead consistent with a transcriptional program associated with epithelial plasticity. Recent studies have increasingly recognized that successful tissue regeneration depends on dynamic and reversible epithelial–mesenchymal state transitions that allow stem cells to adapt to regenerative demands while preserving their long-term

regenerative identity [9, 11, 33–36]. This concept is strongly supported by recent reviews in HFSCs biology, which describe epithelial plasticity and niche-dependent state transitions as central mechanisms governing hair follicle regeneration and tissue remodeling. Such balanced epithelial–mesenchymal plasticity is increasingly recognized as a critical determinant of follicular regeneration, wound re-epithelialization, and tissue remodeling. Therefore, the coordinated elevation of SNAI1 and OVOL2 observed in the present study may reflect a regenerative adaptation process that enhances functional flexibility while potentially retaining features compatible with regenerative competence. This interpretation is further supported by the simultaneous enhancement of cellular migration and metabolic activity, suggesting that He-PAM promotes a regenerative-response state characterized by enhanced functional adaptability and features compatible with regenerative competency.

Collectively, the findings of the present study support a model in which selected He-PAM promotes a regenerative-response profile in HFSCs through the coordinated regulation of three interconnected biological programs: regenerative activation, migratory competence, and epithelial plasticity. Within this framework, plasma-derived reactive species generated in He-PAM may act as bioactive signaling mediators that stimulate molecular programs associated with stem-cell competence and follicular renewal, enhance CXCR4-associated migratory responsiveness, and induce a transcriptional pattern consistent with epithelial-mesenchymal plasticity conducive to tissue remodeling. These coordinated responses are reflected functionally by increased cellular metabolic activity and migration and molecularly by the induction of regeneration-associated transcriptional signatures. Importantly, this integrative response extends beyond changes in cellular metabolic activity alone and suggests that He-PAM may influence fundamental mechanisms governing HFSCs regenerative behavior. This interpretation is in agreement with emerging models of HFSCs regulation, which increasingly view regenerative outcomes as the product of coordinated stem-cell activation, migratory responsiveness, and dynamic cell-state transitions rather than isolated molecular events [9, 11, 33–36]. Given the increasing interest in plasma medicine as a non-thermal, minimally invasive and biologically tunable therapeutic platform, these findings provide new insight into the interaction between plasma-derived bioactive species and hair follicle stem cells. Furthermore, they identify He-PAM as a promising regenerative strategy for modulating key biological processes involved in hair follicle regeneration and potentially other stem-cell-based regenerative applications. Future studies incorporating direct characterization of signaling pathways, protein-level validation, and in vivo models will be valuable for further defining the mechanistic basis and translational potential of these observations.

Several limitations should be considered when interpreting these findings. The present study was designed as a functional and transcriptional investigation and therefore does not establish causal activation of specific signaling pathways. Accordingly, the proposed involvement of Wnt/β-catenin-related regulation, CXCR4-associated migratory signaling, and epithelial–mesenchymal plasticity should be regarded as a biologically supported framework derived from the combined functional and gene-expression data rather than as a demonstrated molecular mechanism. In addition, the reactive-species composition of He-PAM was not directly quantified; therefore, the observed cellular responses cannot be attributed to individual plasma-generated reactive species or to a defined redox dose. The experiments

were performed in vitro and did not directly assess hair-cycle re-entry or follicular regeneration in vivo. Finally, HFSC identity was supported by anatomical isolation from the follicular bulge, cellular morphology, and nestin immunoreactivity, but a broader panel of HFSC-specific markers was not examined. Future studies combining pathway-specific perturbation and signaling analyses with characterization of PAM chemistry and in vivo follicular models will be required to test the proposed regenerative framework and establish the molecular determinants of the He-PAM response.

5. Conclusion

Hair follicle regeneration depends on the coordinated regulation of multiple biological processes that collectively determine stem-cell function and regenerative capacity. Among these, stem-cell activation, migratory responsiveness, and epithelial plasticity have emerged as critical determinants of successful tissue regeneration and follicular renewal. In parallel, plasma medicine has gained increasing attention as a novel regenerative approach capable of modulating cellular behavior through controlled delivery of bioactive reactive species. Understanding how plasma-derived signals influence these fundamental regenerative programs is therefore essential for the rational development of plasma-based therapies. In this context, the present study provides a comprehensive evaluation of the biological responses of hair follicle stem cells to helium plasma-activated medium (He-PAM) by integrating functional assays with molecular analyses of key regenerative processes. Our findings demonstrate that selected He-PAM enhances HFSCs metabolic activity and migratory activity while inducing coordinated transcriptional changes associated with regenerative activation (RUNX1, LGR4, and CCND1), migratory competence (CXCR4), and epithelial plasticity (SNAI1 and OVOL2). Rather than representing isolated molecular alterations, these responses collectively support a model in which He-PAM promotes a regenerative-response profile in HFSCs through the simultaneous regulation of interconnected biological programs governing stem-cell behavior. The observed enhancement of cellular metabolic activity and migration, together with the altered/upregulated expression of genes associated with follicular regeneration, tissue remodeling, and adaptive cell-state transitions, suggests that plasma-derived reactive species may function as bioactive mediators capable of reinforcing regenerative readiness in HFSCs. These findings position He-PAM as a promising plasma-based platform for modulating key regenerative processes relevant to hair follicle biology and regenerative medicine. However, the present work was designed to characterize functional and transcriptional responses rather than to define the precise molecular mechanisms underlying these effects. Therefore, the proposed regenerative framework should be considered a biologically supported model that warrants further mechanistic investigation. Future studies should determine whether the observed transcriptional responses are mediated through signaling networks associated with Wnt/β-catenin activation, CXCR4-related migratory pathways, or regulators of epithelial–mesenchymal plasticity, and should identify the downstream molecular events responsible for the regenerative-response profile associated with He-PAM treatment. Such investigations will be essential for validating the mechanistic basis of the proposed model and further advancing the translational development of plasma-based regenerative therapies.

Declarations

Use of artificial intelligence

During the preparation of this work, the authors used ChatGPT in order to improve language and readability. After using this tool, the authors reviewed and edited the content as needed and take full responsibility for the content of the published article.

Ethics approval and consent to participate

No live animals were used specifically for this study. The animals had originally been bred and used for other research projects unrelated to the present study. The animals used as the source of the post-mortem tissues were from the approved project entitled “Investigating the effect of platelet-rich plasma-derived nanovesicles activated by jet plasma on damage induced by bleomycin in Wistar rat testicular cells,” approved by the Research Ethics Committees of Kharazmi University (Approval ID: IR.KHU.REC.1404.027; Approval Date: May 25, 2025). Following euthanasia, otherwise unused post-mortem tissues, including whisker-pad tissues, were collected for the isolation of hair follicle stem cells for the present study. This approach avoided the use of additional animals and was consistent with the principles of the 3Rs (Replacement, Reduction, and Refinement).

Author Contribution

K. H.: Conceptualization, Methodology, Investigation, Data curation, Formal analysis, Supervision, Writing - review & editing.S. E.: Experimental work, Methodology, Validation, Data curation, Writing - original draft.H. M.: Conceptualization, Formal analysis, Supervision, review & editing.E. A.: Experimental work, Formal analysis, Data interpretation, Supervision, Writing - review & editing.S. P.: Formal analysis, Data interpretation, Supervision, review & editing.E. T.: Experimental work, review & editing.E. R.: Conceptualization, Supervision, review & editing.All authors contributed to the interpretation of the results, critically revised the manuscript, approved the final version of the manuscript, and agreed to be accountable for all aspects of the work.

Acknowledgement

The authors gratefully acknowledge Kavosh Biotech Company for its assistance with real-time PCR analyses. This work has been supported by Center for International Scientific Studies & Collaborations (CISSC), Ministry of Science Research and Technology of Iran, research grant 4020466.

Data Availability

The data used to support the findings of this study are available from the corresponding author upon reasonable request.

References

1. Ahmadi S, et al. Enhanced neural differentiation of epidermal neural crest stem cell by synergistic effect of lithium carbonate and crocin on BDNF and GDNF expression as neurotrophic factors. Iran J Pharm Research: IJPR. 2021;20(2):95.
2. Xing Y-Z, et al. Recent progress in hair follicle stem cell markers and their regulatory roles. World J stem cells. 2024;16(2):126.
3. Chew MW, et al. Hair follicle inspired therapies for wound healing and scar remodelling. Journal of Plastic, Reconstructive & Aesthetic Surgery; 2025.
4. Ito M, et al. Stem cells in the hair follicle bulge contribute to wound repair but not to homeostasis of the epidermis. Nat Med. 2005;11(12):1351–4.
5. Pandamooz S, et al. The influence of cerebrospinal fluid on epidermal neural crest stem cells may pave the path for cell-based therapy. Stem Cell Res Ther. 2013;4(4):84.
6. Lee JH, Choi S. Deciphering the molecular mechanisms of stem cell dynamics in hair follicle regeneration. Exp Mol Med. 2024;56(1):110–7.
7. Zhang B, Chen T. Local and systemic mechanisms that control the hair follicle stem cell niche. Nat Rev Mol Cell Biol. 2024;25(2):87–100.
8. Zou X, et al. TWEAK regulates the functions of hair follicle stem cells via the Fn14-Wnt/β-catenin-CXCR4 signalling axis. Wound Repair Regeneration. 2025;33(3):e70032.
9. Lamouille S, Xu J, Derynck R. Molecular mechanisms of epithelial–mesenchymal transition. Nat Rev Mol Cell Biol. 2014;15(3):178–96.
10. Nieto MA, et al. EMT: 2016. Cell. 2016;166(1):21–45.
11. Watanabe K, et al. OVOL2 induces mesenchymal-to-epithelial transition in fibroblasts and enhances cell-state reprogramming towards epithelial lineages. Sci Rep. 2019;9(1):6490.
12. Hahn O, et al. Cold atmospheric pressure plasma-activated medium modulates cellular functions of human mesenchymal stem/stromal cells in vitro. Int J Mol Sci. 2024;25(9):4944.
13. Schmidt A, Bekeschus S. Redox for repair: cold physical plasmas and Nrf2 signaling promoting wound healing. Antioxidants. 2018;7(10):146.
14. Robert E, Akishev Y, Bauzin J-G, Collet G, Dozias S, Ermolaeva SA, Bocanegra PE, Grillon C, Hajisharifi K, Hocine A, Maaroufi Z, Pouvesle J-M, Prieur F, Rouillard A, Stancampiano A, Vijayarangan V. State of the Art on the Understanding of Plasma Jet Interaction with Skin Tissue Models. Plasma Med, 2025. 15(1).
15. Labérie B, Saugé L, Polesskaya A, Rousseau A, Gautreau AM. Cold atmospheric plasma promotes migration persistence, through induced H_2O_2 and electric field. Biophys J. 2026;125(3):697–708.

16. Roca H, et al. Transcription factors OVOL1 and OVOL2 induce the mesenchymal to epithelial transition in human cancer. PLoS ONE. 2013;8(10):e76773.
17. Subramaniyan B, et al. Role of the CXCR4-LASP1 axis in the stabilization of Snail1 in triple-negative breast cancer. Cancers. 2020;12(9):2372.
18. Wang P, et al. Epithelial-to-mesenchymal transition enhances cancer cell sensitivity to cytotoxic effects of cold atmospheric plasmas in breast and bladder cancer systems. Cancers. 2021;13(12):2889.
19. Watanabe K, et al. Mammary morphogenesis and regeneration require the inhibition of EMT at terminal end buds by Ovol2 transcriptional repressor. Dev Cell. 2014;29(1):59–74.
20. Hoi CS, et al. Runx1 directly promotes proliferation of hair follicle stem cells and epithelial tumor formation in mouse skin. Mol Cell Biol. 2010;30(10):2518–36.
21. Hwang J-H, et al. Non-thermal atmospheric pressure plasma activates Wnt/β-catenin signaling in dermal papilla cells. Sci Rep. 2021;11(1):16125.
22. Ren X, et al. Lgr4 deletion delays the hair cycle and inhibits the activation of hair follicle stem cells. J Invest Dermatology. 2020;140(9):1706–12. e4.
23. Gentile P, et al. Stem cells from human hair follicles: first mechanical isolation for immediate autologous clinical use in androgenetic alopecia and hair loss. Stem cell Invest. 2017;4:58.
24. Mongkolpobsin K, et al. Cold atmospheric microwave plasma (CAMP) stimulates dermal papilla cell proliferation by inducing β-catenin signaling. Sci Rep. 2023;13(1):3089.
25. Mousavi SM, et al. Therapeutic potential of hair follicle-derived stem cell intranasal transplantation in a rat model of ischemic stroke. BMC Neurosci. 2022;23(1):47.
26. Pandamooz S, Chavoshinezhad S, Mostaghel M, Rasekh A, Ghorbani N, Dara M, Pandamooz T, Tanideh N, Salehi MS. Directing Rat Hair Follicle Stem Cells Toward Neuronal Lineage With Enhanced Trophic Factor Expression. Adv Biomedical Res. 2024;13:84.
27. Bell KN. The Role of Krupple-like Factor 5 in Normal Intestinal Homeostasis. University of Cincinnati; 2016.
28. Choi YS, et al. Distinct functions for Wnt/β-catenin in hair follicle stem cell proliferation and survival and interfollicular epidermal homeostasis. Cell Stem Cell. 2013;13(6):720–33.
29. Wang J, et al. Influence of cyclin D1 splicing variants expression on breast cancer chemoresistance via CDK4/CyclinD1-pRB-E2F1 pathway. J Cell Mol Med. 2023;27(7):991–1005.
30. Bekeschus S, von Woedtke T, Emmert S, Schmidt A. Medical gas plasma-stimulated wound healing: Evidence and mechanisms. Redox Biol. 2021;46:102116.
31. Chuang K-T, Chiou S-S, Hsu S-H. Recent advances in transcription factors biomarkers and targeted therapies focusing on epithelial–mesenchymal transition. Cancers. 2023;15(13):3338.
32. Zhang L, et al. SNAI1 promotes epithelial-mesenchymal transition and maintains cancer stem cell-like properties in thymic epithelial tumors through the PIK3R2/p-EphA2 Axis. J Experimental Clin Cancer Res. 2024;43(1):324.

33. Jimenez-Castaño R, Nieto MA. Epithelial-to-mesenchymal transition as a central driver of tumor cell plasticity. Nat Cancer, 2026: pp. 1–16.
34. Ji S, et al. Functional hair follicle regeneration: an updated review. Signal Transduct Target Therapy. 2021;6(1):66.
35. Mao M-Q, et al. Epithelial-mesenchymal interaction in hair regeneration and skin wound healing. Front Med. 2022;9:863786.
36. Solanas G, Benitah SA. Regenerating the skin: a task for the heterogeneous stem cell pool and surrounding niche. Nat Rev Mol Cell Biol. 2013;14(11):737–48.

Figures

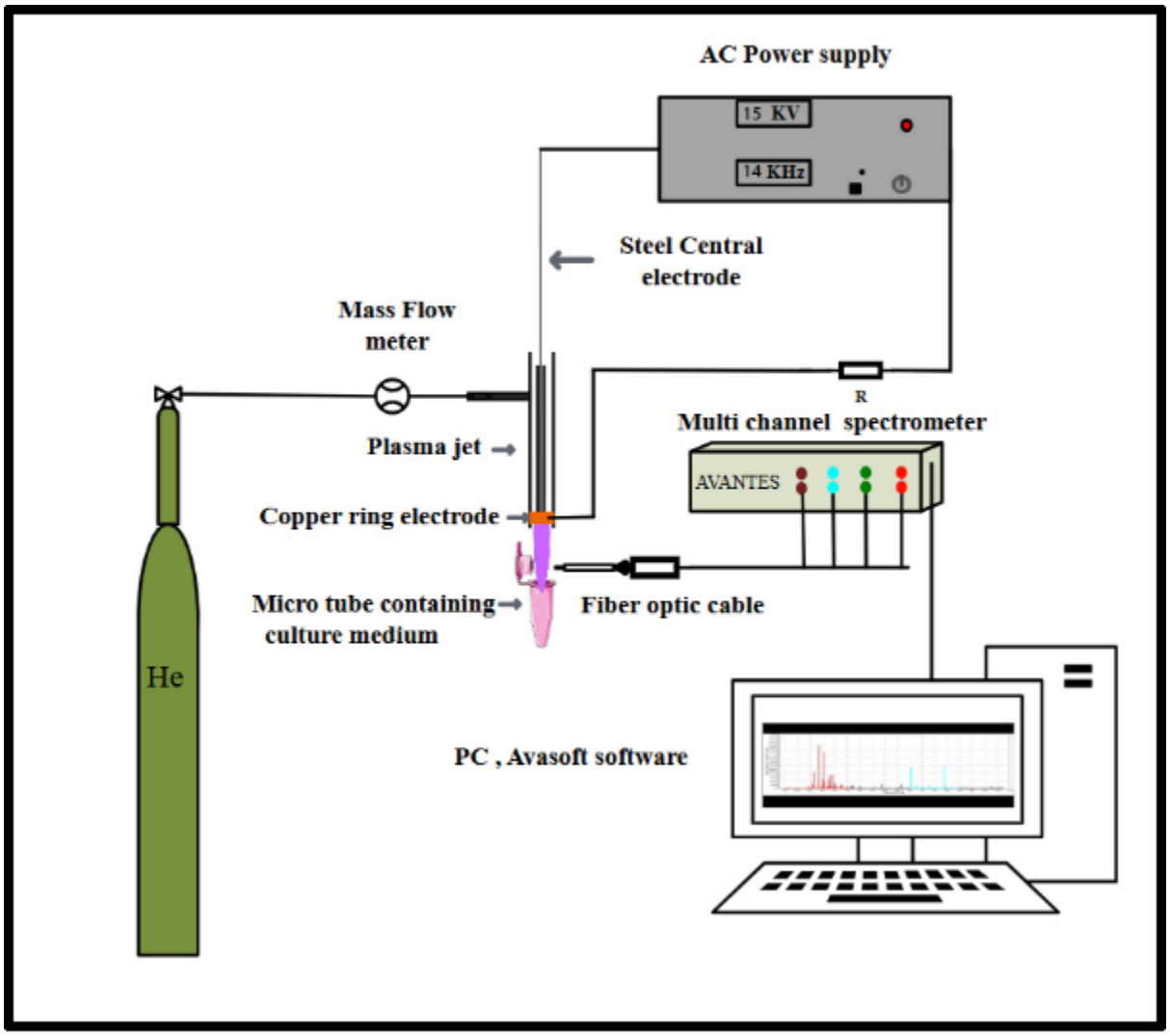


Figure 1

Schematic of helium CAP jet setup for PAM generation.

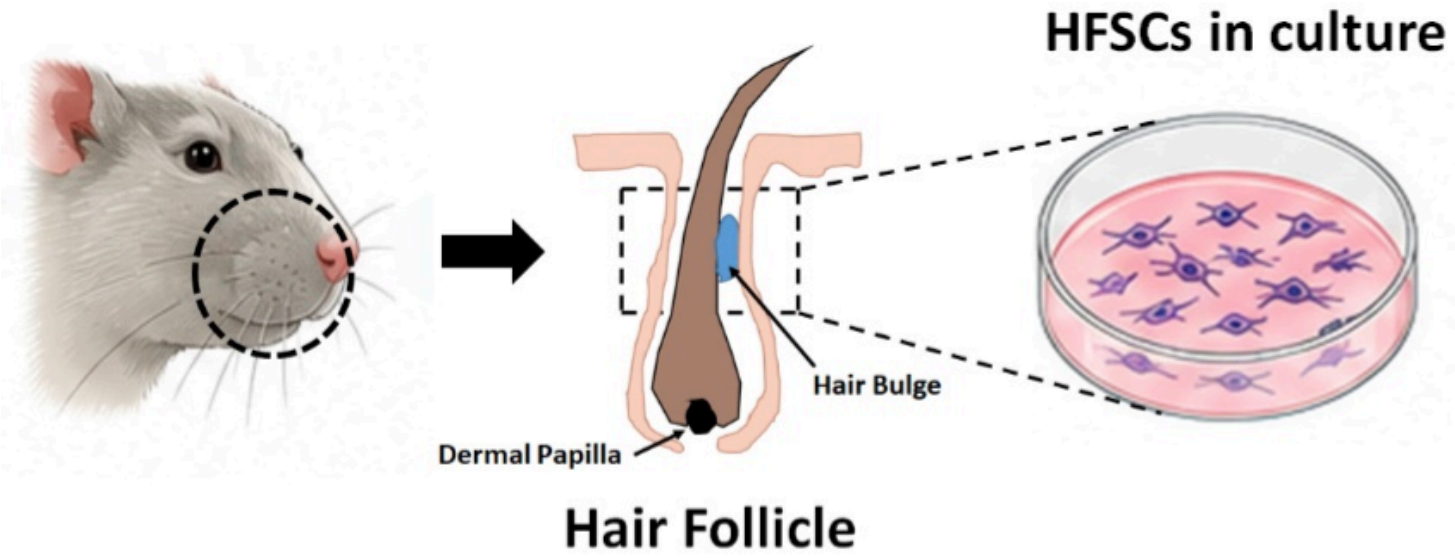


Figure 2

Schematic illustration of hair follicle stem cell (HFSC) isolation and in vitro culture. Hair follicles were microdissected from the rat whisker pad, and the hair bulge region containing HFSCs was isolated. The isolated HFSCs were subsequently cultured in vitro.

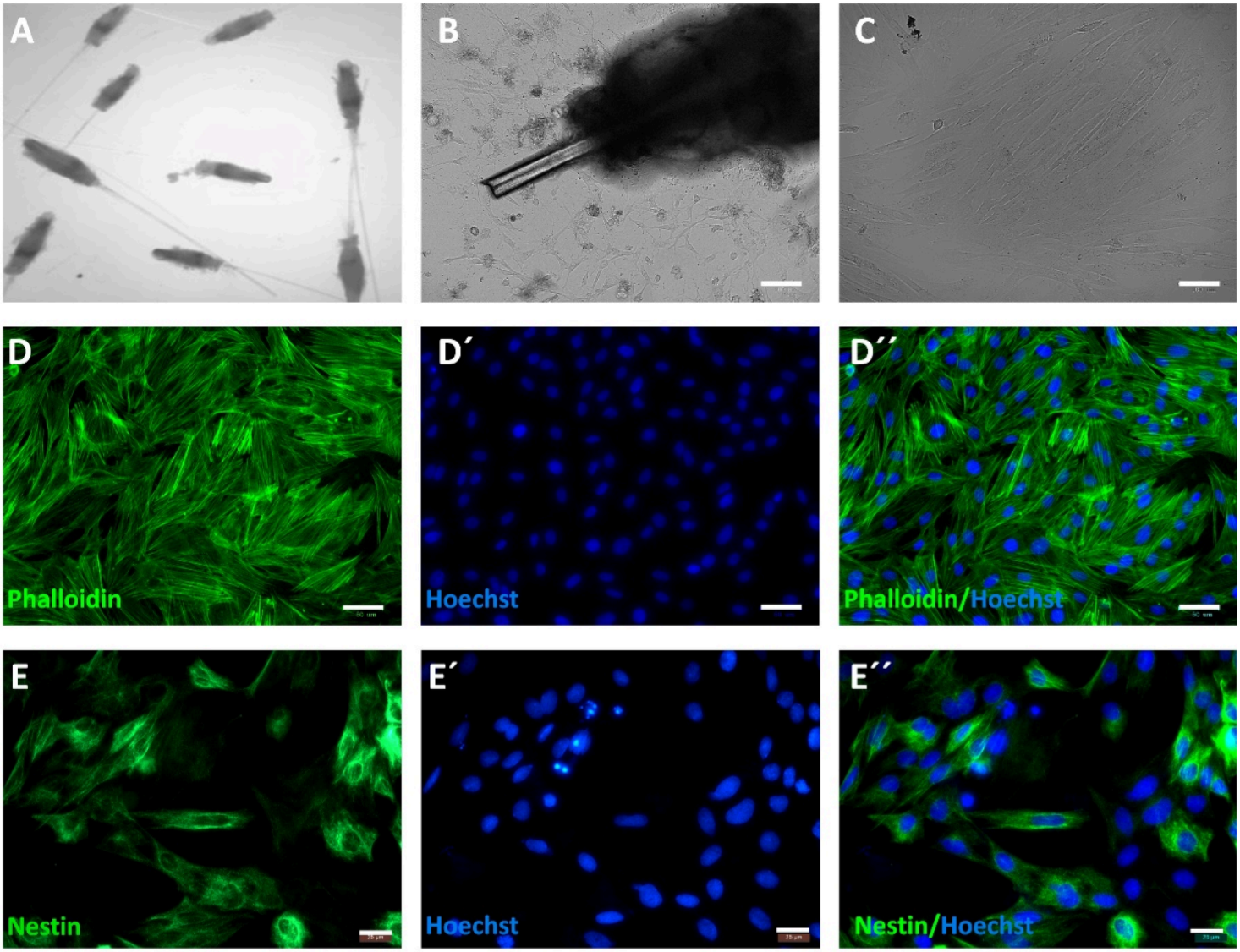


Figure 3

Morphological and immunofluorescence characterization of cultured hair follicle stem cells (HFSCs). (A) Representative whisker hair follicle. (B) Isolated bulge region of the whisker hair follicle, which contains the HFSC niche. (C) Primary cultured HFSCs exhibiting a spindle-shaped, fibroblast-like morphology. (D) F-actin cytoskeleton visualized by phalloidin staining (green). (D') Cell nuclei stained with Hoechst 33342 (blue). (D") Merged image of phalloidin and Hoechst staining. (E) Immunofluorescence staining showing nestin expression (green) in cultured HFSCs. (E') Hoechst 33342 nuclear staining (blue). (E") Merged image demonstrating nestin-positive cultured HFSCs. Scale bars: (B, C) 100 μm; (D–D") 50 μm; (D–E") 25 μm. Images are representative of three independent experiments (n = 3).

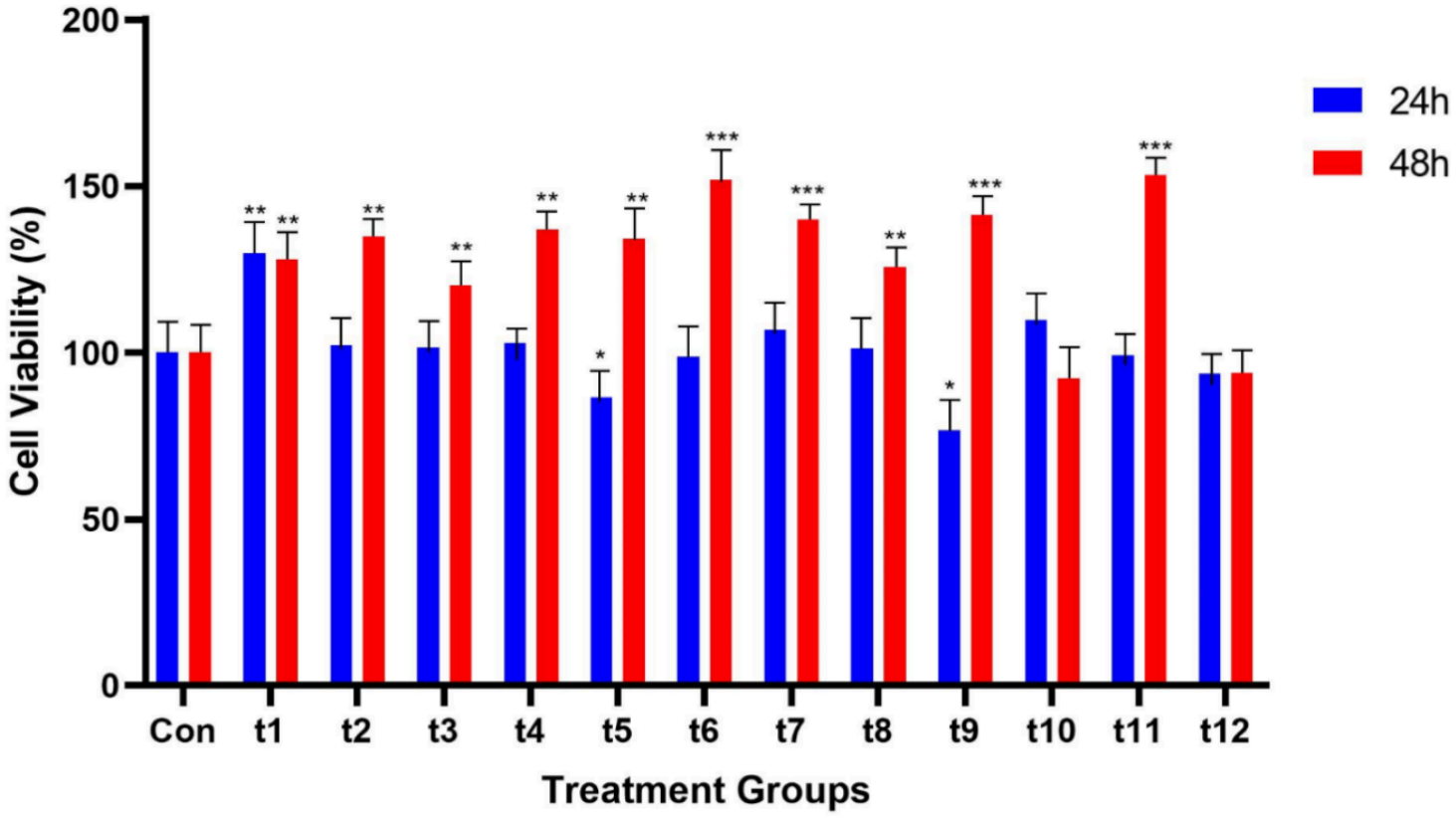


Figure 4

Representative metabolic activity percentages obtained from 24 h and 48 h post-treatment with Helium-PAM by MTT assays. All data represented as mean ± SD (n=3). (*$p < 0.05$, **$p < 0.01$, ***$p < 0.001$)

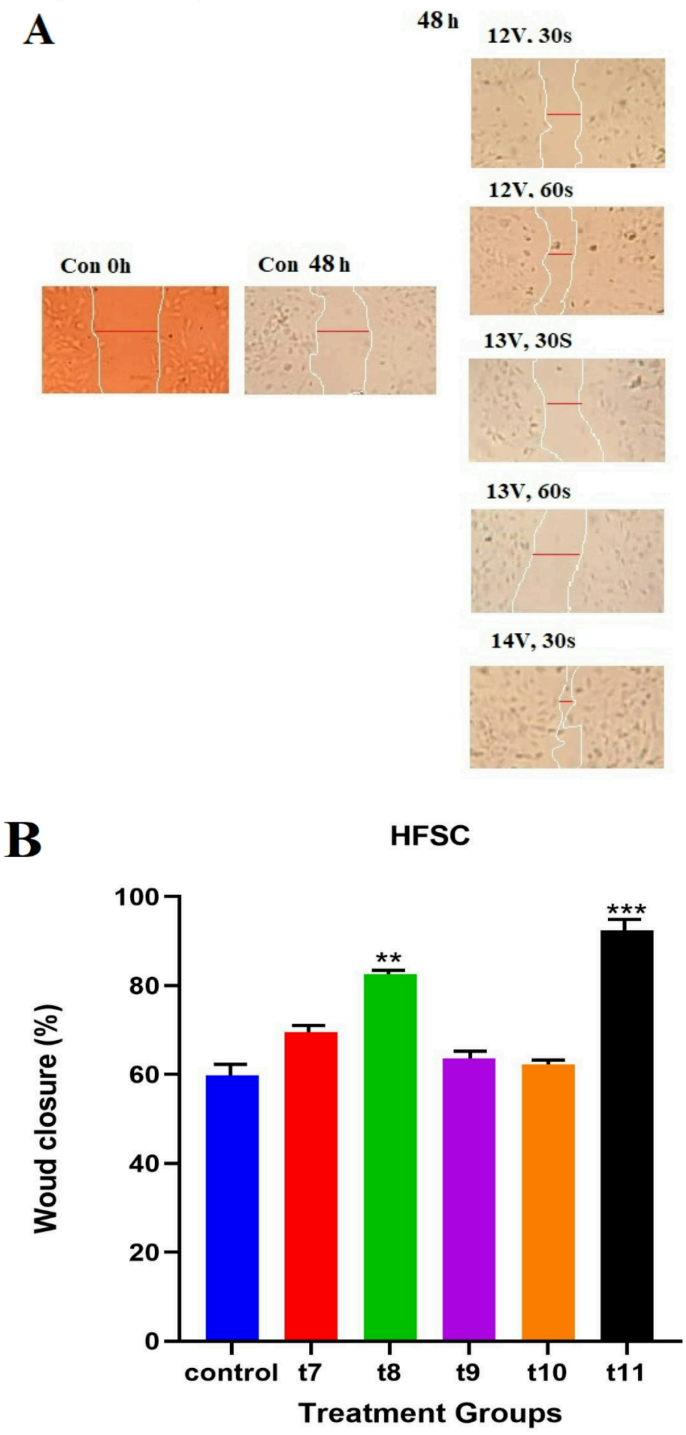


Figure 5

The qualitative and quantitative migratory capacity of HFSCs under exposure with selected PAM. (A) Initial scratch before treatment (control). HFSCs treated with selected voltage and frequency of PAM after 48 h. (B) Quantitative Image J analysis of relative scratch area closure. Untreated cells indicated 59.8 % wound closure, and t8, t11 PAM treated cells as compared with control demonstrated ~92.4%

and 82.6% closure 48h after treatment, respectively. Data are presented as mean ± SD (**p < 0.01, ***p < 0.001. versus control)

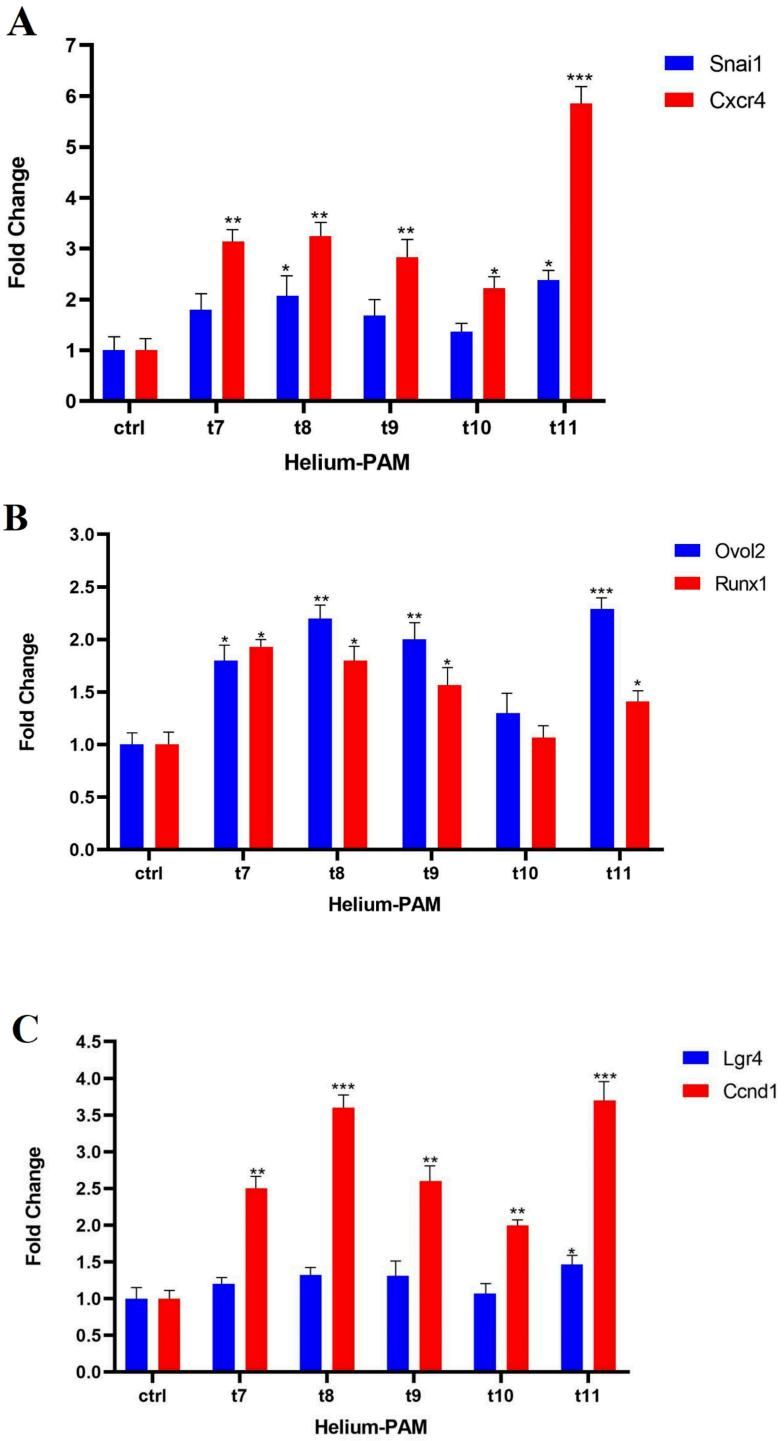


Figure 6

Relative fold change of *SNAI1*, *CXCR4*, *OVOL2*, *RUNX1*, *LGR4*, and *CCND1* genes 48 h after Helium-PAM treatment. Asterisks illustrate the significant differences between PAM treated and control groups (**P <

0.01).